RSC Sustainability

ROYAL SOCIETY OF CHEMISTRY

PAPER

View Article Online
View Journal | View Issue

Cite this: *RSC Sustainability*, 2024, **2**, 2357

Carbon fibers derived from environmentally benign, ethanol-fractionated corn-stover lignin†

Sagar V. Kanhere, ‡ Bronson Lynn, ‡ Mark C. Thies * and Amod A. Ogale §*

Corn stover (CS), the non-grain portion of corn, is among the top three agricultural residues produced globally and the largest in the U.S. CS comprises 75% of all agricultural residues in the U.S. and is an excellent non-food source of sustainable biomass. However, studies of its conversion into carbon fibers are scarce because lignin derived from CS does not possess the needed purity and molecular weight (MW) for precursor fiber spinning and final carbon-fiber properties. Through application of our Aqueous Lignin Purification with Hot Agents (ALPHA) process aqueous ethanol was used to simultaneously clean and fractionate corn-stover lignin to produce a liquefied precursor. Fractionation enabled higher MW components to be used for successful dry-spinning of thin CS precursor fibers. Furthermore, the higher MW also increased glass transition temperature of the precursor lignin, which reduced stabilization time to 9 hours, an impressive four-fold improvement as compared to prior studies using unfractionated corn-stover lignins. Carbon fibers from higher MW lignin fractions displayed a tensile strength of 1.0 ± 0.1 GPa, double that of previous carbon fibers derived from corn-stover lignin. These carbon fibers possess a specific modulus of 48 GPa (g^{-1} cm^3), about 50% greater than that of glass fibers, establishing their novelty as a low-cost reinforcing material suitable for potential applications such as ultrahigh temperature thermal insulation, electrostatic dissipation, and ablative composites.

Received 21st March 2024
Accepted 3rd July 2024

DOI: 10.1039/d4su00138a

rsc.li/rscsus

Sustainability spotlight

Due to ethical concerns over the use of food-grade cellulose for biofuel and industrial products, non-food sources such as corn stover represent a truly world-wide sustainable option. Corn stover is the agricultural residue produced from non-grain components of corn and comprises 75% of all agricultural residues in the United States. Biorefining the corn stover can yield about 20% lignin, which can be either burned for its calorific value or valorized for higher-value applications. This study focused on the use of corn-stover-derived lignin to produce carbon fibers that possess tensile and transport properties comparable to that of current, rayon-based carbon fibers, which find application in ultrahigh temperature insulation and ablative composite applications. This research aligns with UN SDGs # 9, 12, and 15 by successfully producing carbon fibers from sustainable corn-stover lignin, ensuring responsible consumption of nonfood natural resources that also does not lead to forest depletion.

1 Introduction

Lignin has the potential to be a low-cost and sustainable precursor for carbon fibers because of its low-cost, abundance, and high carbon content.[1–3] To date, most research has focused on Kraft lignin,[4,5] produced as a by-product of the pulp and paper industry. However, the non-grain portion of corn, corn stover (CS), is among the top three agricultural residues produced globally and the largest in the United States. Due to ethical concerns regarding usage of food-grade corn grain as a feedstock for biorefinery, there is an incentive to use corn stover as the feedstock in biorefineries. Conversion of the polysaccharide portion (70–75%) of CS to bioethanol in these biorefineries has been technically successful, but low profitability is hindering their commercial success. However, lignin is produced as a waste stream of the process and can be burned for its calorific value or, preferably, valorized into high value products. Thus, the utilization of CS lignin (comprising ~20% of CS) for materials applications, such as carbon fibers, is frequently proposed as the path forward to commercially viable lignocellulosic biorefineries.[4,6,7]

In most of the prior lignin-based, carbon-fiber (CF) studies, the precursor fibers are produced *via* melt-spinning, using lignin with low molecular weights. To reduce the impurities, the starting raw lignin is dissolved in a solvent (or solvent mixture) and is then filtered to remove the solid impurities. The resulting soluble lignin fraction is thus a lower molecular weight (MW) portion of the lignin. Unfortunately, this leads to unstable fiber

Center for Advanced Engineering Fibers and Films, Department of Chemical Engineering, Clemson University, Clemson, SC 29634, USA. E-mail: ogale@clemson.edu; mcths@clemson.edu

† Electronic supplementary information (ESI) available. See DOI: https://doi.org/10.1039/d4su00138a

‡ These authors contributed equally.

§ Lead contact.

spinning, impractically long stabilization times, and carbon fibers with poor mechanical properties.[8,9] In contrast, higher MW lignins typically start to degrade before melting, making it impossible to process using melt-spinning methods.

Considering the abundance of corn stover as a biomass stream, it is reported that lignin valorization into high value products would make an overall biorefining process economical.[10,11] Carbon fibers are one such high value product, highly sought after for various composite reinforcement applications. A prior study has reported on the production of carbon fibers from CS lignin.[12] Raw CS lignin recovered *via* organosolv processing (supplied by ADM) was purified with neat methanol, which reduced the ash content of the soluble (and thus lower MW) portion from 6.1 to 0.27 wt%. However, this lignin fraction still had to undergo two-step acetylation in order to generate a spinnable precursor. Subsequently, 40 hours were required to stabilize the fibers at the optimum acetylation level, with light fiber fusion occurring. The resulting carbon fibers had a tensile strength and modulus of 454 ± 98 MPa and 62 ± 14 GPa, respectively. Similar tensile properties were reported with switchgrass lignin-based CFs,[13,14] but no other systematic studies using only grass lignins have been reported in the literature.

The Thies group[15–17] has developed the Aqueous Lignin Purification with Hot Agents (ALPHA) process, which exploits the liquid–liquid equilibrium that can form when hot aqueous organic solvents are mixed with raw lignins, to simultaneously purify, fractionate, and solvate lignins.[16] ALPHA was first applied to a softwood Kraft lignin using hot aqueous acetic acid (AcOH) as the solvent, with the higher MW, cleaned, and liquefied-lignin phase being isolated in a single equilibrium stage. This solvated lignin–AcOH–H_2O phase was then dry-spun into fibers, producing the highest tensile strength (1.39 ± 0.2 GPa) carbon fibers ever from neat lignins.[18]

ALPHA process was also applied to a hybrid poplar (HP) hardwood lignin that had been recovered from the raw biomass *via* alkaline pretreatment.[19] However, the first ALPHA stage had to be dedicated to purification, which reduced the impurities in HP lignin from 4 wt% (notably higher than we see in Kraft lignin) to 0.1 wt%. Ultraclean lignin fractions were generated, with increasing molecular weight giving a corresponding increase in glass transition temperature (T_g). Using the highest HP lignin MW fraction, a five-fold increase in stabilization rate and a carbon fiber tensile strength of 1.1 ± 0.2 GPa were obtained, double that previously reported.[19]

For above studies, it is noted that melt-spining of fibers was not possible because the higher molecular weight fractions do not melt. Instead, the precursor lignin fibers were produced by dry-spinning. Dry-spinning of lignin is now an established route and has been documented in various prior literature studies over the past many years.[18–22] Hardwood as well as softwood have been used in conjunction with solvents such as acetone, acetic acid, ethanol, and dimethyl sulfoxide. In the current study, the innate advantage of dry-spinning is that bioethanol can be used for purification/fractionation of feed lignin, and then again as the solvent for subsequent for dry-spinning of lignin solution.

Unfortunately, corn-stover lignin tends to possess elevated levels of impurities (particularly carbohydrates, as grasses contain a higher proportion of carbohydrates than woody biomasses). Additionally, the molecular weight of the CS feed lignin is dependent on pretreatment and recovery processes. Impurity content and molecular weight of lignin are crucial parameters that influence the resulting carbon fiber properties. However, there is lack of understanding regarding how molecular weight and impurities in CS lignin affect spinning, stabilization, and properties of CS-lignin-based carbon fibers.

Therefore, the overall goal of this study was to develop carbon fibers from ALPHA-processed corn stover lignin that was chemically unmodified. The low impurity and high MW CS-lignin fractions were obtained using ethanol, which is an environmentally benign solvent that itself can be produced from corn stover.[23] The specific objectives of this study were to (i) produce low impurity ALPHA-fractionated CS lignin samples and dry-spin these into precursor fibers using aqueous ethanol as the primary solvent, (ii) convert CS lignin fibers into carbon fibers, and (iii) study the structure–property relationships of the resulting carbon fibers.

2 Experimental

2.1 ALPHA solvents employed

Absolute ethanol (EMPARTA ACS analytical reagent, Supelco) was purchased from VWR. Deionized water was produced from an in-house Culligan system paired with a Milli-Q reference system (Millipore Z00QSV0WW). These solvents were mixed in various proportions to create the desired ALPHA solvent compositions.

2.2 Generation of clean, higher MW lignin fractions *via* ALPHA

Lignin was recovered from the CS biomass using an alkaline pretreatment process described in detail in a prior study.[24] Because this recovered lignin contained a high level of impurities (*i.e.*, 10% polysaccharides and 3% metals measured as ash), it first had to be cleaned using an ALPHA purification stage as illustrated in Fig. 1. In particular, the lignin was mixed with an 80/20 wt/wt% ethanol/water solution at a solvent-to-lignin mass ratio (S/L) of 3 : 1 for 30 min in a Parr reactor at 60 (CS9.4K) or 75 °C (CS15K & CS20K). Two liquid phases formed, one being a liquefied-lignin phase (L1) concentrated with essentially all of the impurities, and the other being a solvent-rich phase (S1) into which ~80% of the lignin dissolved. The reactor contents were then vacuum-filtered to ensure complete separation of the insoluble impurities from the solvent-rich phase. Details of the purification step are given elsewhere.[24]

Multistage ALPHA was then used to isolate three, higher MW fractions from S1 for conversion into carbon fibers. The first fraction, denoted as CS9.4K (*i.e.*, with a number-average MW of 9.4 kDa), was the liquefied-lignin phase (LLΦ) that precipitated when the ethanol concentration in S1 (originally at 80 wt%) was reduced from 55 to 45 wt% ethanol by water addition at ambient temperature (about 25 °C). Previous work[24] had shown

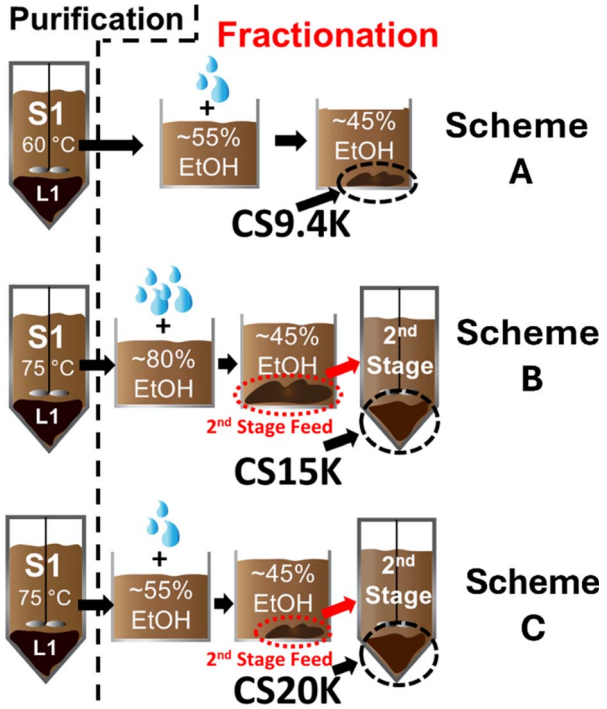

Fig. 1 Schematic of the ALPHA purification and fractionation process used to produce the lignin precursors.

that this cut would precipitate out the highest MW lignins; the lower MW lignins that precipitated from 80 to 55 wt% ethanol were not used.

The second lignin fraction, CS15K, was obtained by first adding water to S1 at ambient temperature to reduce the ethanol concentration from 80 to 45 wt%, precipitating out an LLΦ. A second ALPHA fractionation stage was then performed on this LLΦ (after drying it to obtain the needed mass balances), by mixing it with a 42% EtOH/water solution at a solvent : lignin (S : L) ratio of 9 : 1 and 65 °C for 30 min, which precipitated out the LLΦ denoted as CS15K.

The third and highest MW fraction was obtained by also applying a 2nd ALPHA stage to the equivalent of CS9.4K produced from an S1 phase purified at 75 °C instead of 60 °C. The same procedure as for the 2nd stage of CS15K was used, except that a 6 : 1 S : L ratio and 37% EtOH were used to precipitate out the LLΦ of CS20k. Higher temperatures for the second ALPHA stages of CS15K and CS20K were selected with the objective of precipitating out only the higher MWs in the LLΦ and solubilizing most of the lower MW lignins in the solvent phase.

2.3 Analytical characterization of lignins

Ash content of the starting bulk lignin and of the lignin fractions was determined *via* thermogravimetric analysis (TGA), performed on a TA Instruments Q5000 under air, using a 10 °C min^{-1} ramp rate from room temperature to 750 °C. All mass loss had ceased by 730–750 °C.

Polysaccharides (a.k.a. sugars) content of the lignins was determined using an adaptation to the NREL/TP-510-42618 method for structural carbohydrate content determination, as detailed elsewhere.[17] The absolute molecular weight (MW) of the lignin fractions was determined *via* GPC-MALS (DAWN, Wyatt Technologies). Gel permeation chromatography (GPC) was used for the separation of the lignin moieties by molecular weight, with the above MALS serving as the detector. The complete MW procedure is detailed in our earlier study.[24] Glass transition temperatures of the various lignin fractions isolated by ALPHA were determined by differential scanning calorimetry (DSC), using an MDSC 2920 calorimeter (TA Instruments). Heating–cooling cycles were carried out under an inert (helium) atmosphere.

2.4 Dry-spinning of lignin fractions into precursor fibers

Lignin fractions CS9.4K, CS15K, and CS20K (identified in terms of their number-average molecular weight) were dry-spun from ethanol/water solutions at 50–70 °C. Interestingly, these conditions are similar to those where they formed as LLΦ's during the liquid–liquid phase splits induced by ALPHA. After mixing, the homogenous lignin–ethanol–water solution was transferred into a preheated barrel fitted with a spinneret and a sintered metal filter. Dry spinning was carried out in a batch spinning unit (Alex James Associates, Greenville, SC) operated under constant throughput conditions and attached to a 12-hole spinneret.

2.5 Stabilization and carbonization of lignin fibers

As-spun fibers were subjected to oxidative stabilization under constant load in a programmable forced-air convection oven (Memmert GmbH + Co, Schwabach, Germany). This is an important step where the precursor material gets crosslinked and prevents melting during subsequent heat treatment.[25] Stabilized fibers were carbonized using Astro 1000 (Thermal Technology LLC) furnace under constant length.

Preliminary analysis showed that when fibers were carbonized at 750 °C, there was inadequate carbon layer formation. On the other hand, at a carbonization temperature of 1500 °C, gross defects were observed on the lateral surface of the carbon fibers that are detrimental for CF strength. These observations are consistent with trends reported in prior studies, even for high performance PAN-based carbon fibers, that indicate the existence of a nominally optimal carbonization temperature (*i.e.*, not too low but also not too high).[26] For the current CS-lignin based fibers, 1000 °C was found to be an adequately high carbonization temperature, and was used for all results reported in this study.

2.6 Carbon fiber characterization

To analyze the microstructure, micrographs of fiber cross-sections and lateral surfaces were obtained using Regulus 8230 Field Emission Scanning Electron Microscope. Raman analysis of carbon fibers was conducted using Renishaw inVia Raman scope with a laser wavelength of 785 nm and laser power of 25 mW focused using 50× lens at 10% power and calibrated using Si crystal at 520 cm^{-1}.

Wide-angle X-ray diffraction experiments were conducted on carbon fibers using a Rigaku SmartLab powder diffractometer, using CuK$_\alpha$ radiation (0.15406 nm), and a Hypix3000 detector. The data from Raman and XRD were analysed using Wire3.4 (Renishaw) software and smoothed in Origin software (Originlab Corp.) using the Savitzky–Golay method.

Carbon fibers were tensile-tested by following ASTMD 3822 standard using the MTI-1K tensile testing frame. Compliance correction was performed using the ASTM C 1557-03 method to obtain accurate tensile modulus results.[27] Electrical resistivity of the carbon fibers was calculated from the resistance measured across 10 mm long carbon fibers.[28,29] Accurate cross-sectional area of the fibers was measured from SEM images of the individual filament cross-section; nominal/equivalent diameters calculated from the measured cross-sectional areas are reported for reference purposes.

3 Results and discussion

3.1 Lignin purification, fractionation, and characterization

As displayed in Table 1, impurities (*i.e.*, ash and sugars) in the CS Feed Lignin exceeded 12%. Grass-based lignins are notorious for having the highest impurities levels among the three types of lignin.[30–32] In previous work with hardwood[17] and softwood[33] lignins, impurities levels were one-quarter and one-tenth, respectively, of the levels seen with CS lignin. Thus, the three schemes depicted in Fig. 1 were used to both clean and fractionate the CS feed lignin to purity and MW levels such that they would be expected to serve as acceptable precursors for carbon fibers.

In all three schemes, the first stage shown is for purification. Here, most impurities were removed in the denser, liquefied-lignin phase L1 that formed during the liquid–liquid phase split, with most of the lignin (containing few impurities) dissolving in solvent phase S1. Conditions for each purification stage (see Section 2.2), to both maximize lignin solubility/MW and minimize impurities solubility in S1, were selected based both on previous work with hybrid poplar lignin[17] and from preliminary experiments with CS feed lignin. For Scheme A, our goal was to isolate the highest MW lignin fraction using but a single equilibrium stage. Previous work[17,24] has shown that when the ethanol concentration was reduced from 55 to 45 wt%, the highest MW portion of the lignin feed would precipitate out as a liquefied-lignin phase (LLΦ), circled in the figure as "CS9.4K". Table 1 indicates that the increase in MW (to 9.4 kDa) was relatively modest; on the other hand, more than an order-of-magnitude reduction in impurities was obtained *vs.* the feed lignin.

Thus, a 2nd fractionation stage was added in Scheme B to isolate a higher MW fraction. For the 1st fractionation stage, all LLΦ samples that precipitated were collected (circled as "2nd stage feed") when water was added to S1 after Purification to reduce the ethanol concentration in S1 from 80 to 45%. This cut included both the medium and higher MW lignins. A 2nd ALPHA fractionation stage using a 37% EtOH/water solution at 65 °C and a S/L ratio of 9 : 1 was then used both to purify and extract away the lower and med MW lignins, leaving the higher MW's in the 2nd stage LLΦ. As displayed in Table 1, CS15K was the purest CS fraction isolated, and the MW was double that of the CS feed. Note that the yield and the MW increased over CS9.4K, due to the larger "pool" of lignin fed to the 2nd stage, which included lignins that precipitated from 80 to 55% ethanol.

In Scheme C, purification was carried out at a higher temperature of 75 °C to extract as much lignin from the feed as possible. For the first fractionation stage, only the highest MW portion of the lignin was isolated, which precipitated out in the 55 to 45% EtOH range (as shown in Scheme A). That LLΦ then served as the "2nd stage feed" to the 2nd ALPHA fractionation stage, which operated at 65 °C, with a solvent feed of 42 wt% EtOH and an S/L ratio of 6/1. Notably, Table 1 indicates that this last scheme also generated a high-purity lignin, one with almost triple the MW of the lignin feed.

3.2 Corn stover lignin fibers

3.2.1 Dry-spinning of precursor fibers. Using the same ethanol/water solvent system employed for ALPHA fractionation, liquified lignin solutions were subjected to dry spinning. Due to reduced ash and sugars impurities, all three fractions of CS lignin could be extruded through the spinneret capillaries and drawn into thin fibers on the roll as shown in Fig. 2(a). Dry spinning is a process where fiber drawing and solvent evaporation happen simultaneously.[20,21,34–39] Therefore, the temperature of the lignin solution is a crucial factor for successful spinning of a given solution. SEM micrographs of CS lignin fibers dry-spun at a low temperature of about 55 °C are shown in Fig. 2(c). These precursor fibers did not have cracks on the surface but had only mild crenulations on the surface. As the solution temperature increased beyond a solution temperature of 65 °C, fibers became too brittle to draw down and resulted in fiber breakage. This is likely due to rapid solvent out-diffusion leading to the formation of a hard skin that did not allow

Table 1 Properties of lignin-fraction precursors prepared *via* the ALPHA process

Lignin fraction ID	Number average molecular weight (kDa)	Glass transition temperature T_g (°C)	Ash content (wt%)	Sugars (wt%)	Yield (% of feed lignin)
Feed lignin	7.3	—	2.9	9.5	—
CS9.4K	9.4	154	0.25	0.3	17
CS15K	14.8	160	0.05	0.1	20
CS20K	20.3	173	0.07	0.2	15

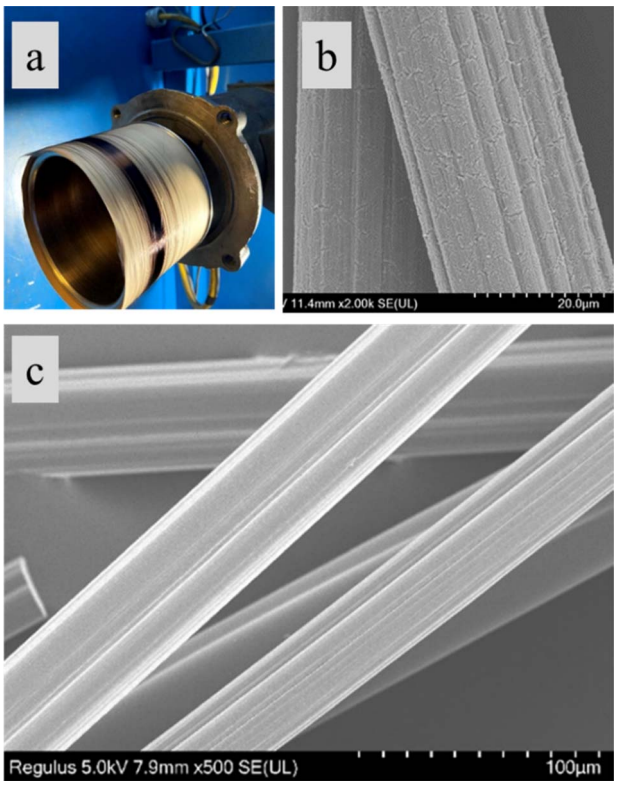

Fig. 2 Dry-spinning of CS-lignin: (a) fibers (dark brown) collected on the draw-down roll; (b) SEM micrograph of as-spun fibers showing cracks on the lateral surface when spun at higher temperatures; and (c) SEM micrograph of as-spun fibers with crenulations on the surface.

fiber extension due to the dried outer skin. As shown in Fig. 2(b), cracks were observed on the lateral surface of the as-spun fibers spun at a spinning temperature of 70 °C. Thus, the optimum dry spinning solution temperature range was found to be between 50 and 60 °C, conveniently close to that of the ALPHA fractionation temperature.

The highest drawdown ratio, an indicator of successful fiber formation, achieved for cleaner CS20K lignin was 6, whereas for higher impurity containing CS9.4K it was only 4. Drawdown increased with solution temperature until the temperature reached 60 °C, after which drawdown was poor and fibers were brittle. The fiber surface dried out faster with an increase in temperature, hindering fiber drawdown, which is consistent with literature modeling and experimental observations.[34,35]

The spinning temperature impacts not only the drawdown but also the fiber shape. As shown in Fig. 3(a), fibers spun at 67 °C have sharp curvature with doubly convex surfaces forming a sharp crevice. As the solution temperature was reduced to 62 °C, the fiber surface and crenulations became smoother as displayed in Fig. 3(b). Fibers spun at the lowest temperature of 57 °C, displayed in Fig. 3(c), did not show any significantly curved surfaces. Thus, for dry-spinning performed at higher temperatures, fiber cross-section displayed sharper curvature and crenulations on the fiber surface. However, at temperatures lower than 50 °C, phase separation of the lignin from solution occurred, making it impossible to produce fibers.

Above observations are consistent with those reported in prior dry-spinning studies.[22,34,36] Although crenulations lead to increased surface area for matrix bonding in composites, sharp crenulations can also lead large stress concentrations as compared to more circular shaped fibers.[40] Thus, to produce fibers without sharp crenulations, moderately high solution temperatures are desirable.

Overall, the dry-spinning of fractionated CS lignin solution was successfully conducted at temperatures between 50–60 °C for all three fractions. As-spun fiber diameter ranged from 20 to 35 µm (nominal), with the highest drawdown ratio being 6.

3.2.2 Thermo-oxidative stabilization. To enable conversion of as-spun CS lignin fibers into carbon fibers, CS fibers must be "stabilized" (*i.e.*, crosslinked within). The stabilization time depends on lignin glass transition temperature and reactivity. During the stabilization process, it is critical that fibers retain their shape and do not fuse. Thus, the heating rate needs to be slow enough such that the fiber (oven) temperature remains below the glass transition temperature of lignin throughout the stabilization step.

As displayed in Table 1, as the molecular weight of the fractionated lignin increased from 9.4 kDa to 15 kDa to 20 kDa, the glass transition temperature increased from 154 °C to 160 °C to 173 °C, respectively. Thus, as expected, glass transition temperature increased with an increase in molecular weight of CS lignin. This confirms that the fractionation of CS lignin led to an increase in glass transition temperature, consistent with prior observations.[12,19,41]

Lower molecular weight CS lignin (CS9.4K and CS15K) fibers could be stabilized without any observable fiber fusion using a slow 0.25 °C min^{-1} ramp rate. A faster rate of 0.5 °C min^{-1} led to lignin fiber fusion because fiber temperature exceeded (or

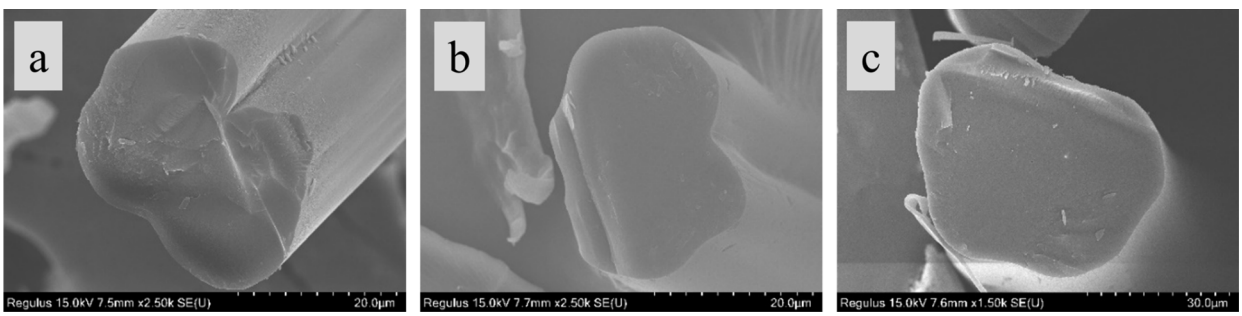

Fig. 3 SEM micrographs of CS20K fibers dry-spun at temperatures of (a) 67 °C (b) 62 °C, and (c) 57 °C.

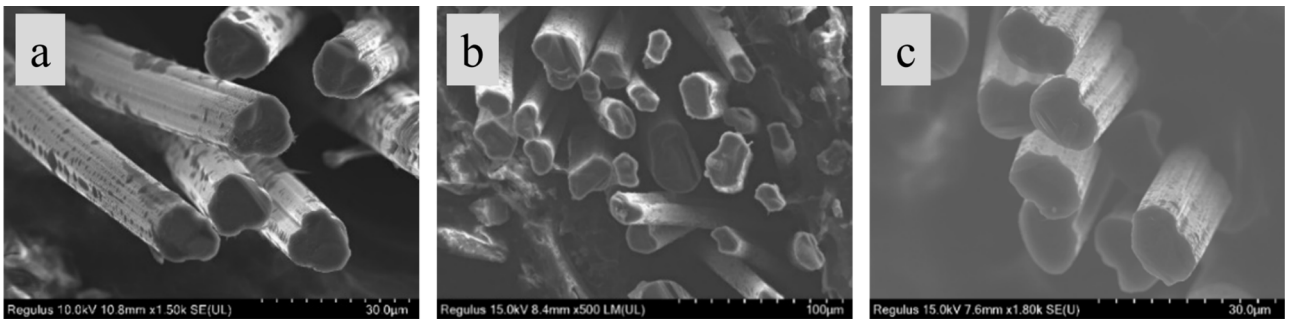

Fig. 4 SEM micrographs of the cross-section of CFs carbonized at 1000 °C and produced using (a) CS9.4K; (b) CS15K (c) CS20K.

approached) its T_g and the lignin softened. Then the increased molecular mobility allowed self-diffusion of lignin segments at the fiber surfaces, which led to partial sticking of fibers to each other. It is emphasized that precursor fiber fusion is extremely detrimental to resulting carbon fiber strength because the fusion spots create surface defects that lead to reduction of fiber strength. In contrast, the highest molecular weight lignin (CS20K) could be stabilized using rates as fast as 0.5 °C min^{-1} because its T_g was higher to begin with, and stayed higher than the fiber temperature even at the higher heating rate. Thus, the stabilization time required for CS20K was only 9 h, whereas it was double (18 hours) for CS9.4K and CS15K.

Increased T_g of precursor lignin due to fractionation allows lignin to remain in a glassy state at higher temperatures. Therefore, the stabilization reaction can take place at a higher temperature without fiber fusion for CS lignin with higher T_g. Furthermore, the rate of reaction has an exponential dependence on the temperature, drastically reducing the time required for a complete lignin crosslinking reaction.

As compared to the stabilization times reported for stabilization of corn-stover lignin in prior literature studies,[12] the current results represent a four-fold reduction in time, *i.e.*, a four times faster process, a requirement for the overall carbon fiber process to be economical and scalable. Thus, a stabilization time of 9 h achieved in this study (and the first report of a grass lignin stabilization time under 10 h) was enabled by an increase in glass transition temperature due to increased molecular weight *via* ALPHA lignin fractionation.

3.2.3 Carbonization. Stabilization extent and precursor suitability is important for successful carbonization process. Fig. 4(a–c) show representative SEM micrographs of fiber cross-sections of CFs produced from different lignin fractions. As evident from the SEMs, CFs did not possess any detectable holes in the cross-section. Carbon fibers also did not show any evidence of fusion with neighboring fibers, underscoring the successful stabilization process. Thus, ALPHA-fractionated, CS-lignin-based fibers were successfully carbonized at 1000 °C without fusion or gross defects.

The carbon yield of these CS-lignin precursors, as measured by thermogravimetric analysis (following ASTM 1131-20 standard), were nominally 34.6, 35.3 and 37.4 wt%, (differences statistically not significant). This is not surprising because these fractions were obtained using the ALPHA process, which is a separation technique. Because ALPHA fractionation does not involve any chemical reaction of lignin, the chemical moieties in various fractions were not expected to be different, and the carbon content too was not expected to be different. Overall, these yields were consistent with similar values of 35 wt% reported in prior literature studies for lignins, but slightly lower than that observed for other precursors, namely, PAN (45 wt%) and mesophase pitch (75 wt%).[42]

3.3 Carbon fiber characteristics

3.3.1 Raman spectroscopy. Fig. 5 displays Raman spectra of CFs produced from CS9.4K-, CS15K-, and CS20K-lignin fractions and carbonized at 1000 °C. The G and D peaks were nominally located at 1580 and 1320 cm^{-1}, consistent with prior results on lignin-based carbon materials.[43] The I_G/I_D ratios, an indication of carbon layer order, were 0.24 ± 0.05, 0.24 ± 0.08 and 0.23 ± 0.05 for the CFs produced from CS9.4K-, CS15K-, and CS20K-lignin grades, respectively. These ratios did not show any statistically significant difference among CFs produced using different CS lignin molecular weights. As compared with I_d/I_g of PAN- or pitch-based carbon fibers (0.7 and 1.0, respectively[29,44]), current I_G/I_D ratios are significantly smaller, indicating a lack of significant graphitic (crystalline) development. The corresponding predicted in-plane crystallite size $L_{a\|}$ values using the correlation proposed by Cançado *et al.*[45] were estimated to be 18 ± 4, 18 ± 6, 17.9 ± 4, nm for the CFs produced from CS9.4K-, CS15K-, and CS20K-lignin grades, respectively. These values are

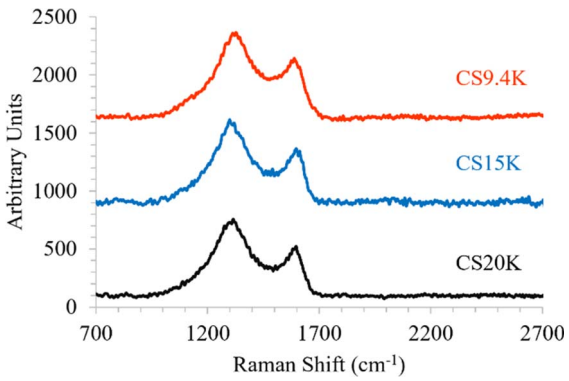

Fig. 5 Raman spectra of CFs carbonized at 1000 °C from various CS lignin fractions.

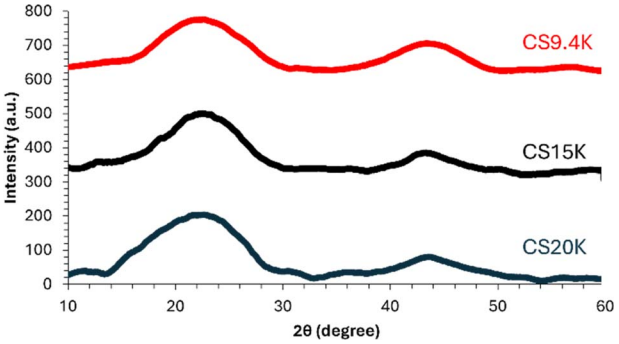

Fig. 6 WAXD diffractograms of CFs carbonized at 1000 °C and derived from various CS lignin fractions.

generally consistent with those reported in previous studies on softwood kraft lignin fibers (20–24 nm).[39] However, these in-plane crystallite lengths are much smaller than those found in highly graphitic mesophase pitch-based carbon fibers (up to 160 ± 5 nm).[29]

3.3.2 Wide-angle X-ray diffraction (WAXD). Fig. 6 displays wide-angle X-ray diffraction spectra of CFs carbonized at 1000 °C from different CS lignin fractions. The accuracy of 2-theta location was validated using a NIST-grade Si standard; d_{002} was observed at 28.4°, which is consistent with the specification.[29,39] For various lignin precursor fractions (CS9.4K, CS15K, and CS20K), CFs carbonized at 1000 °C showed a broad peak centered around 23°, indicating very low graphitic development as a consequence of significant disorder in the carbon structure. The d_{002} spacing was estimated using Bragg's law to be 0.385, 0.378 and 0.382 nm for CFs produced from CS9.4K, CS15K and CS20K lignin, respectively.[46] This value is not only much larger than the *d*-spacing of 0.3354 nm observed for graphitic carbon but also larger than 0.343 nm observed for turbo-stratic carbon layers in PAN-based CFs. From these WAXD spectra, the stacking height (L_c) was estimated to be about 0.7 nm using Scherrer's equation, much smaller than CFs from PAN and pitch precursors (about 4 nm, and 20 nm, respectively[29,47]). This small stacking height of layer planes (equivalent to only a few carbon layers) is consistent with prior literature results[39,43] as well as the Raman results presented in the prior section that indicated a low level of graphitic development.

3.3.3 Tensile properties. Tensile strength of CS-lignin based carbon fibers is displayed in Table 2. Both CS9.4K and CS15K-based CFs with an equivalent diameter of 14.0 ± 1.3 and 13 ± 2 μm (no statistically significant difference) displayed a tensile strength of only 0.6 ± 0.1 GPa. CS20K-based CFs of similar diameter (12 ± 1 μm) possessed a higher tensile strength of 1.0 ± 0.1 GPa. A few individual filaments displayed a tensile strength as high as 1.2 GPa. Compliance corrected modulus of CS20K-based CFs carbonized at 1000 °C was measured at 82 ± 8 GPa. This modulus value is the highest ever reported for carbon fibers derived from grass lignins, and also rivals that of E- and S-glass fibers (70–85 GPa).[48]

The density of CS-lignin-based CFs was measured to be about 1.7 g cm^{-3}, which is comparable to PAN-based carbon fibers (T300, 1.76 g cm^{-3}) but much lower than highly graphitic mesophase pitch-based carbon fibers (2.1 g cm^{-3}).[49,50] Thus, the specific strength of the current carbon fibers was determined to be nominally 0.6 GPa (g^{-1} cm^3). The specific modulus was 48 GPa (g^{-1} cm^3), which is about 50% higher than that of glass fibers. It is noted that at 1.7 g cm^{-3}, current CFs are almost 30–40% lighter than glass fibers, whose density is about 2.6 g cm^{-3}.[48] Both specific tensile properties of CS lignin-based CFs are higher than those of conventional structural materials such steel[51,52] [specific strength ≈0.1–0.3 GPa (g^{-1} cm^3), modulus ≈18–25 GPa (g^{-1} cm^3)] and aluminum[53] [specific strength ≈0.2 GPa (g^{-1} cm^3), modulus ≈28 GPa (g^{-1} cm^3)].

3.3.4 Electrical resistivity. Electrical resistivity values of CS-lignin-based CFs carbonized at 1000 °C are also listed in Table 2. CS9.4K-based CFs has a higher electrical resistivity of 77 ± 15 μΩ.m, which moderately reduced to 49 ± 6 μΩ.m for CS20K-based CFs. The electrical resistivity values are similar to those reported for other lignin-based carbon fibers.[39,43] However, these electrical resistivity values are much higher than those of pitch- or PAN-based carbon fibers.[50,54] Higher electrical resistivity values (*i.e.*, lower electrical conductivity) are generally consistent with the disordered carbon structure indicated by Raman spectroscopy and X-ray diffraction results. Due to the disordered carbon structure of CS lignin-based CFs, electrical resistivity is comparable to that of rayon-based CFs. Rayon-based carbon fibers have a tensile strength of 1.1 GPa and electrical resistivity ranging between 45 and 55 μΩ m.[55,56] The relatively high values of electrical resistivity (*i.e.*, low conductivity) of current corn-stover-based carbon fibers are similar to those of rayon-based CFs and suggest potential application as reinforcing fibers for high temperature thermal insulation and ablative composites.[55,57]

Although these CS-based carbon fibers were less electrically conducting than graphitic ones, they are still electrically conducting. This is a major advantage over glass fibers that are electrically nonconducting. Thus, the current carbon fibers can potentially be used in applications such as battery electrodes, electrostatic dissipation (ESD) and electromagnetic interference (EMI) shielding, when glass fibers cannot. Further, the use of nonfood agricultural by-products as the starting precursor is the

Table 2 Summary of CS-lignin-based carbon fiber characteristics

Precursor lignin ID	CF equivalent diameter (μm)	CF tensile strength (GPa)	Electrical resistivity (μΩ m)
CS9.4K	14 ± 1	0.6 ± 0.1	77 ± 15
CS15K	13 ± 2	0.6 ± 0.1	65 ± 10
CS20K	12 ± 1	1.0 ± 0.1	49 ± 6

major environmental benefit of the carbon fibers developed in this research.

4 Conclusions

This study has established for the first time that if CS lignin (which in its raw state is laden with impurities and is of relatively low MW) is cleaned/fractionated *via* the ALPHA process using ethanol/water solutions, the resulting higher-MW lignin fractions can be dry-spun into precursor fibers using the same renewable solvent system. Interestingly, solids content and temperatures used for dry-spinning are similar to those used to isolate the lignin fractions *via* ALPHA.

By doubling the molecular weight of the lignin fraction *via* ALPHA, the total time required for stabilization was reduced by 50% (*i.e.*, from 18 to 9 h), a major accomplishment. Carbon fibers were successfully carbonized at 1000 °C, *i.e.* carbonized fibers do not show any evidence of fusion or gross defects. Furthermore, a higher molecular weight precursor lignin generated by ALPHA not only improved the stabilization rate but also led to a higher tensile strength of 1.0 ± 0.1 GPa, which represents almost 100% improvement over that previously reported for CS-lignin-based CFs, in which the starting lignin had to be chemically modified (acetylated).[12] The compliance-corrected modulus of the CS-lignin-based CFs, 82 + 8 GPa, is on par with that of E-glass fibers, a common reinforcement glass fiber grade.[58–62]

Microstructural analysis showed that CS-lignin-based CFs have a significantly disordered carbon structure, yielding an electrical resistivity of 49 ± 6 μΩ m, similar to that of rayon-based carbon fibers. Although the tensile strength of carbon fibers produced in the current study is not high enough for use in high-strength structural composites, these fibers have been produced from sustainable sources and possess environmental benefits, as discussed above.[62,63] They are of value in potential applications such as ultrahigh temperature thermal insulation or for non-structural applications such as battery electrodes and ESD- and EMI-shielding, where strength is not the critical property.

Data availability

The data supporting this article have been included as ESI.†

Author contributions

Conceptualization, M. C. T. and A. A. O.; methodology, S. V. K. and B. L.; validation, S. V. K. and B. L.; investigation, S. V. K. and B. L.; writing – original draft S. V. K. and B. L.; writing – review and editing S. V. K., A. A. O., B. L. and M. C. T.; supervision A. A. O. and M. C. T.; funding acquisition M. C. T. and A. A. O.

Conflicts of interest

There are no conflicts to declare.

Acknowledgements

This work was supported by the U.S. Department of Energy, Bioenergy Technologies Office (BETO) under agreement No. EE0008502. Partial equipment support was provided by the Center for Advanced Engineering Fibers and Films. The authors would like acknowledge help received from Villő Bécsy-Jakab and Dr David Hodge at Montana State University for the pretreatment and recovery of corn-stover lignin, Dr Colin MacMillen for XRD, Kim Ivey for DSC, Oreoluwa Agede for TGA and Elijah Taylor, Mark Walsh, Charlton Hill, Courtney Owens, Blake Reardon, and Andrew Demchak for their assistance with the processing and characterization of carbon fiber.

References

1 H. Mainka, O. Täger, E. Körner, L. Hilfert, S. Busse, F. T. Edelmann and A. S. Herrmann, Lignin – An alternative precursor for sustainable and cost-effective automotive carbon fiber, *J. Mater. Res. Technol.*, 2015, **4**(3), 283–296.

2 A. A. Ogale, M. Zhang and J. Jin, Recent advances in carbon fibers derived from biobased precursors, *J. Appl. Polym. Sci.*, 2016, **133**(45), 43794, **https://onlinelibrary.wiley.com/doi/epdf/10.1002/app.43794**.

3 D. A. Baker and T. G. Rials, Recent advances in low-cost carbon fiber manufacture from lignin, *J. Appl. Polym. Sci.*, 2013, **130**, 713–728.

4 S. Sethupathy, G. Murillo Morales, L. Gao, H. Wang, B. Yang, J. Jiang, J. Sun and D. Zhu, Lignin valorization: Status, challenges and opportunities, *Bioresour. Technol.*, 2022, **347**, 126696.

5 L. Dessbesell, M. Paleologou, M. Leitch, R. Pulkki and C. Xu, Global lignin supply overview and kraft lignin potential as an alternative for petroleum-based polymers, *Renewable Sustainable Energy Rev.*, 2020, **123**, 109768.

6 M. Langholtz, M. Downing, R. Graham, F. Baker, A. Compere, W. Griffith, R. Boeman and M. Keller, Lignin-Derived Carbon Fiber as a Co-Product of Refining Cellulosic Biomass, *SAE Int. J. Mater. Manuf.*, 2014, **7**, 115–121.

7 V. K. Garlapati, A. K. Chandel, S. P. J. Kumar, S. Sharma, S. Sevda, A. P. Ingle and D. Pant, Circular economy aspects of lignin: Towards a lignocellulose biorefinery, *Renewable Sustainable Energy Rev.*, 2020, **130**, 109977.

8 S. Kanhere, Doctoral dissertation, Clemson University, 2022.

9 R. M. Paul and A. Naskar, *Low-Cost Bio-Based Carbon Fibers for High Temperature Processing*, GrafTech International, Brooklyn Heights, OH, United States, 2017.

10 K. Huang, P. Fasahati and C. T. Maravelias, System-Level Analysis of Lignin Valorization in Lignocellulosic Biorefineries, *iScience*, 2020, **23**, 100751.

11 D. Bbosa, M. Mba-Wright and R. C. Brown, More than ethanol: a techno-economic analysis of a corn stover-ethanol biorefinery integrated with a hydrothermal liquefaction process to convert lignin into biochemicals, *Biofuels, Bioprod. Biorefin.*, 2018, **12**, 497–509.

12 W. Qu, J. Liu, Y. Xue, X. Wang and X. Bai, Potential of producing carbon fiber from biorefinery corn stover lignin with high ash content, *J. Appl. Polym. Sci.*, 2018, **135**, 45736.
13 O. Hosseinaei, D. P. Harper, J. J. Bozell and T. G. Rials, Improving Processing and Performance of Pure Lignin Carbon Fibers through Hardwood and Herbaceous Lignin Blends, *Int. J. Mol. Sci.*, 2017, **18**, 1410.
14 A. Attwenger, MS thesis, University of Tennessee, Knoxville, 2014.
15 A. S. Klett, P. V. Chappell and M. C. Thies, Recovering ultraclean lignins of controlled molecular weight from Kraft black-liquor lignins, *Chem. Commun.*, 2015, **51**, 12855–12858.
16 M. C. Thies, A. S. Klett and D. A. Bruce, Solvent and recovery process for lignin, *US Pat.*, US10053482B2, 2018, **https://patents.google.com/patent/US10053482B2/en**.
17 G. Tindall, B. Lynn, C. Fitzgerald, L. Valladares, Z. Pittman, V. Bécsy-Jakab, D. Hodge and M. Thies, Ultraclean hybrid poplar lignins via liquid–liquid fractionation using ethanol–water solutions, *MRS Commun.*, 2021, **11**, 692–698.
18 J. Jin, J. Ding, A. Klett, M. C. Thies and A. A. Ogale, Carbon Fibers Derived from Fractionated–Solvated Lignin Precursors for Enhanced Mechanical Performance, *ACS Sustain. Chem. Eng.*, 2018, **6**, 14135–14142.
19 S. V. Kanhere, G. W. Tindall, A. A. Ogale and M. C. Thies, Carbon fibers derived from liquefied and fractionated poplar lignins: The effect of molecular weight, *iScience*, 2022, **25**, 105449.
20 M. Zhang and A. A. Ogale, Effect of temperature and concentration of acetylated-lignin solutions on dry-spinning of carbon fiber precursors, *J. Appl. Polym. Sci.*, 2016, **133**(45), 43663, **https://onlinelibrary.wiley.com/doi/abs/10.1002/app.43663**.
21 M. Zhang and A. A. Ogale, Carbon fibers from dry-spinning of acetylated softwood kraft lignin, *Carbon*, 2014, **69**, 626–629.
22 S. Otani, Y. Fukuoka, B. Igarashi and K. Sasaki, Method for producing carbonized lignin fiber, *US Pat.*, US3461082A, 1969, **https://patents.google.com/patent/US3461082A/en**.
23 P. Trivedi, R. Malina and S. R. H. Barrett, Environmental and economic tradeoffs of using corn stover for liquid fuels and power production, *Energy Environ. Sci.*, 2015, **8**, 1428–1437.
24 B. Lynn, Z. A. Pittman, V. Bécsy-Jakab, D. B. Hodge and M. C. Thies, Fractionation and purification of a high-impurity, alkaline-pretreated, corn stover lignin with simple renewable solvents, *Sep. Purif. Technol.*, 2024, 126924.
25 E. I. Akpan, in *Sustainable Lignin for Carbon Fibers: Principles, Techniques, and Applications*, ed. E. I. Akpan and S. O. Adeosun, Springer International Publishing, Cham, 2019, pp. 325–352.
26 D. D. L. Chung, *Carbon Fiber Composites*, Butterworth-Heinemann, Boston, MA, 1994.
27 ASTM International, *ASTM C1557-03, Standard Test Method for Tensile Strength and Young's Modulus of Fibers*, West Conshohocken, PA, 2003.
28 S. V. Kanhere, V. Bermudez and A. A. Ogale, in *CAMX 2020 – Composites and Advanced Materials Expo: Combined Strength. Unsurpassed Innovation*, 2020.
29 V. Bermudez, Doctoral dissertation, Clemson University, 2019.
30 F. F. de Menezes, J. Rencoret, S. C. Nakanishi, V. M. Nascimento, V. F. N. Silva, A. Gutiérrez, J. C. del Río and G. J. de Moraes Rocha, Alkaline Pretreatment Severity Leads to Different Lignin Applications in Sugar Cane Biorefineries, *ACS Sustainable Chem. Eng.*, 2017, **5**, 5702–5712.
31 C. Nitsos, R. Stoklosa, A. Karnaouri, D. Vörös, H. Lange, D. Hodge, C. Crestini, U. Rova and P. Christakopoulos, Isolation and Characterization of Organosolv and Alkaline Lignins from Hardwood and Softwood Biomass, *ACS Sustainable Chem. Eng.*, 2016, **4**, 5181–5193.
32 A. Ekielski and P. K. Mishra, Lignin for Bioeconomy: The Present and Future Role of Technical Lignin, *Int. J. Mol. Sci.*, 2021, **22**, 63.
33 O. Agede and M. C. Thies, Purification and Fractionation of Lignin via ALPHA: Liquid–Liquid Equilibrium for the Lignin–Acetic Acid–Water System, *ChemSusChem*, 2024, **17**, e202300989.
34 I. Brazinsky, A. G. Williams and H. L. LaNieve, The dry spinning process: Comparison of theory with experiment, *Polym. Eng. Sci.*, 1975, **15**, 834–841.
35 Z. Gou and A. J. McHugh, Dry Spinning of Polymer Fibers in Ternary Systems: Part II: Data Correlation and Predictions, *Int. Polym. Process.*, 2004, **19**, 254–261.
36 M. Zhang, Doctoral dissertation, Clemson University, 2016.
37 Z. Gou and A. J. McHugh, A comparison of Newtonian and viscoelastic constitutive models for dry spinning of polymer fibers, *J. Appl. Polym. Sci.*, 2003, **87**, 2136–2145.
38 Y. Imura, R. M. C. Hogan and M. Jaffe, in *Advances in Filament Yarn Spinning of Textiles and Polymers*, ed. D. Zhang, Woodhead Publishing, 2014, pp. 187–202.
39 J. Jin, Doctoral dissertation, Clemson University, 2018, **https://tigerprints.clemson.edu/all_dissertations/2256**.
40 E. E. Carapella, M. W. Hyer, O. H. Griffin and H. G. Maahs, Micromechanics of Crenulated Fibers, *J. Compos. Mater.*, 1994, **28**, 1322–1346.
41 Q. Sun, R. Khunsupat, K. Akato, J. Tao, N. Labbé, N. C. Gallego, J. J. Bozell, T. G. Rials, G. A. Tuskan, T. J. Tschaplinski, A. K. Naskar, Y. Pu and A. J. Ragauskas, A study of poplar organosolv lignin after melt rheology treatment as carbon fiber precursors, *Green Chem.*, 2016, **18**, 5015–5024.
42 C. D. Warren, *Carbon Fiber Precurosors and Conversion*, Oak Ridge TN, 2016, **https://www.energy.gov/sites/prod/files/2016/09/f33/fcto_h2_storage_700bar_workshop_3_warren.pdf**.
43 W. J. Sagues, A. Jain, D. Brown, S. Aggarwal, A. Suarez, M. Kollman, S. Park and D. S. Argyropoulos, Are lignin-derived carbon fibers graphitic enough?, *Green Chem.*, 2019, **21**, 4253–4265.
44 X. Qian, X. Wang, J. Zhong, J. Zhi, F. Heng, Y. Zhang and S. Song, Effect of fiber microstructure studied by Raman spectroscopy upon the mechanical properties of carbon fibers, *J. Raman Spectrosc.*, 2019, **50**, 665–673.

45 L. G. Cançado, K. Takai, T. Enoki, M. Endo, Y. A. Kim, H. Mizusaki, A. Jorio, L. N. Coelho, R. Magalhaes-Paniago, M. A. Pimenta, R. Magalhães-Paniago and M. A. Pimenta, General equation for the determination of the crystallite size La of nanographite by Raman spectroscopy, *Appl. Phys. Lett.*, 2006, **88**, 163106.

46 S. A. Speakman, *Estimating Crystallite Size Using XRD*, MIT Center for Materials Science and Engineering, Boston MA, **http://prism.mit.edu/xray**.

47 N. Meek and D. Penumadu, Nonlinear elastic response of pan based carbon fiber to tensile loading and relations to microstructure, *Carbon*, 2021, **178**, 133–143.

48 *E-Glass Fiber Data Sheet, Generic*, **https://www.matweb.com/search/DataSheet.aspx?MatGUID=d9c18047c49147a2a7c0b0bb1743e812**, accessed 15 September 2022.

49 Mitsubishi Chemical Corporation Carbon Fiber and Composites, *DIALEAD Dataset*, **https://www.m-chemical.co.jp/carbon-fiber/pdf/tow/CarbonFiberTow(ContinuousFiber)20230227.pdf**, accessed June, 20, 2024.

50 *T300 Standard Modulus Carbon Fiber Data Sheet*, Toray Composite Materials America, 2018.

51 W. Wang, B. Liu and V. Kodur, Effect of Temperature on Strength and Elastic Modulus of High-Strength Steel, *J. Mater. Civ. Eng.*, 2013, **25**, 174–182.

52 Y. He, K. Yang, W. Qu, F. Kong and G. Su, Strengthening and toughening of a 2800-MPa grade maraging steel, *Mater. Lett.*, 2002, **56**, 763–769.

53 A. Villuendas, A. Roca and J. Jorba, Change of Young's Modulus of Cold-Deformed Aluminum AA 1050 and of AA 2024 (T65): A Comparative Study, *Mater. Sci. Forum*, 2007, **539–543**, 293–298.

54 S. Kanhere, V. Bermudez and A. Ogale, Transport properties of carbon fibers derived from petroleum-based mesophase pitch with modified transverse microstructures for enhanced tensile strength, *SAMPE-Composites and Advanced Materials Expo*, SAMPE Virtual, 2020, **https://www.nasampe.org/store/viewproduct.aspx?ID=17556324**.

55 W. Gindl-Altmutter, I. Czabany, C. Unterweger, N. Gierlinger, N. Xiao, S. C. Bodner and J. Keckes, Structure and electrical resistivity of individual carbonised natural and man-made cellulose fibres, *J. Mater. Sci.*, 2020, **55**, 10271–10280.

56 P. Morgan, *Carbon Fibers and Their Composites*, CRC Press, 2005.

57 R. C. Rossi and W. C. Wong, in *AIAA Conference of Missile Sciences*, 1995.

58 J. Ahmad, R. A. González-Lezcano, A. Majdi, N. Ben Kahla, A. F. Deifalla and M. A. El-Shorbagy, Glass Fibers Reinforced Concrete: Overview on Mechanical, Durability and Microstructure Analysis, *Materials*, 2022, **15**, 5111.

59 K. Palanikumar, M. Ramesh and K. Hemachandra Reddy, Experimental Investigation on the Mechanical Properties of Green Hybrid Sisal and Glass Fiber Reinforced Polymer Composites, *J. Nat. Fibers*, 2016, **13**, 321–331.

60 Y. R. Atewi, M. F. Hasan and E. Güneyisi, Fracture and permeability properties of glass fiber reinforced self-compacting concrete with and without nanosilica, *Constr. Build. Mater.*, 2019, **226**, 993–1005.

61 A. B. Kizilkanat, N. Kabay, V. Akyüncü, S. Chowdhury and A. H. Akça, Mechanical properties and fracture behavior of basalt and glass fiber reinforced concrete: An experimental study, *Constr. Build. Mater.*, 2015, **100**, 218–224.

62 F. Hermansson, S. Heimersson, M. Janssen and M. Svanström, Can carbon fiber composites have a lower environmental impact than fiberglass?, *Resour., Conserv. Recycl.*, 2022, **181**, 106234.

63 Y. Xu, Y. Liu, S. Chen and Y. Ni, Current overview of carbon fiber: Toward green sustainable raw materials, *Bioresearch*, 2020, **15**, 7234–7259.